Applications in Engineering Science 3 (2020) 100014

Contents lists available at ScienceDirect

Applications in Engineering Science

journal homepage: www.elsevier.com/locate/apples

Experimental characterization of pull-in parameters for an electrostatically actuated cantilever

A. Sorrentino, G. Bianchi*, D. Castagnetti, E. Radi

Dipartimento di Scienze e Metodi dell'Ingegneria, Università di Modena e Reggio Emilia, Via G. Amendola 2, 42122 Reggio Emilia, Italy

ARTICLE INFO

Keywords:
Pull-In instability
MEMS
Cantilever actuators
Experimental validation

ABSTRACT

MEMS-NEMS applications extensively use micro-nano cantilever structures as actuation system, thanks to their intrinsically simple end efficient configuration. Under the action of an electrostatic actuation voltage the cantilever deflects, until it reaches the maximum value of the electrostatic actuation voltage, namely the pull-in voltage. This limits its operating point and is a critical issue for the switching of the actuator. The present work aims to experimentally measure the variation of the pull-in voltage and the tip deflection for different geometrical parameters of an electrostatically actuated cantilever. First, by relying on a nonlinear differential model from the literature, we designed and built a macro-scale cantilever switch, which can be simply adapted to different configurations. Second, we experimentally investigated the effect of the free length of the suspended electrode, and of the gap from the ground, on the pull-in response. The experimental results always showed a close agreement with the analytical predictions, with a maximum relative error lower that 10% for the pull-in voltage, and a relative difference lower than 18% for the pull-in deflection.

1. Introduction

This work experimentally investigates the pull-in instability of an electrostatically actuated cantilever beam, which reproduces the typical behavior of the micromechanical switching blocks in MEMS and NEMS applications. The interesting properties of the MEMS devices typically arise from the behavior of the active parts, which, in most cases, are in the forms of cantilevers (Ke et al., 2005; Espinosa et al., 2006). Cantilever beams represent a very efficient solution in the field of MEMS applications (Ionescu, 2015; Zhang et al., 2014). The fundamental component of MEMS and NEMS cantilever devices is a suspended electrode above a fixed conductive substrate and actuated by a voltage difference, which exploits the switching of the flexible electrode between two stable positions (Loh and Espinosa, 2012; Chuang et al., 2010). A physical schematic of the MEMS cantilever beam is show in Fig. 1a, where V_{out} and V_{PI} represent the input voltage applied to the micro-beams and the critical pull-in voltage of the system, respectively. Under the action of the electrostatic forces, the flexible micro-cantilever beam deflects towards the substrate (Fig. 1b) thus increasing the electrostatic force between the two electrodes. It comes that the flexible micro-cantilever becomes unstable, and then, at a critical voltage, named the pull-in voltage, the flexible electrode tip pulls-in onto the substrate (Fig. 1-c), thus creating an electrical connection (Knapp and De Boer, 2002; Gorthi et al., 2006). This actuation scheme has been used in many micro-nano scale devices, such as manipulators, tweezers, accelerometers, pressure sensors, memory devices and energy harvesting systems (Spaggiari et al., 2016). The purpose of these components is to process very fast communications (Eric Garfunkel, 2009) in addition to a smarter and very smaller micro-nano devices (Noghrehabadi et al., 2013). The planar technologies represent the most common actuation mechanism used in micro-nano MEMS devices giving their tiny size, low mass and high resonance frequency as well as the electrostatic actuation (Passian and Thundat, 2011). Since the critical pull-in voltage defines the operating voltage and power dissipation of the system, it must be accurately determined.

The first works on the nonlinear pull-in phenomenon are reported by Taylor (1968) and Wickstrom and Davis (1967) dating in the late 1960s. In the last years, Dequesnes et al. (2002) propose the use of parametrized continuum model that aims to calculate the pull-in voltages in nanoelectromechanical switches. The work of Ramezani et al. (2008) focused on a general analytical method for the calculation of the pull-in instability in nano-cantilevers under electrostatic actuation. In particular, the work investigates a typical micro-nano actuator composed by a flexible beam and of a fixed plate with a very small gap separation between the two electrodes. The electromechanical behavior of the cantilever beams can be described by fourth-order nonlinear ordinary differential equation (ODE) and no exact solution can be obtained (Ramezani et al., 2008). In this case, the modeling of the nonlinear response of the device must

* Corresponding author.
E-mail addresses: andrea.sorrentino@unimore.it (A. Sorrentino), giovanni.bianchi@unimore.it (G. Bianchi), davide.castagnetti@unimore.it (D. Castagnetti), enrico.radi@unimore.it (E. Radi).

https://doi.org/10.1016/j.apples.2020.100014
Received 6 September 2020; Accepted 10 September 2020
Available online 12 September 2020

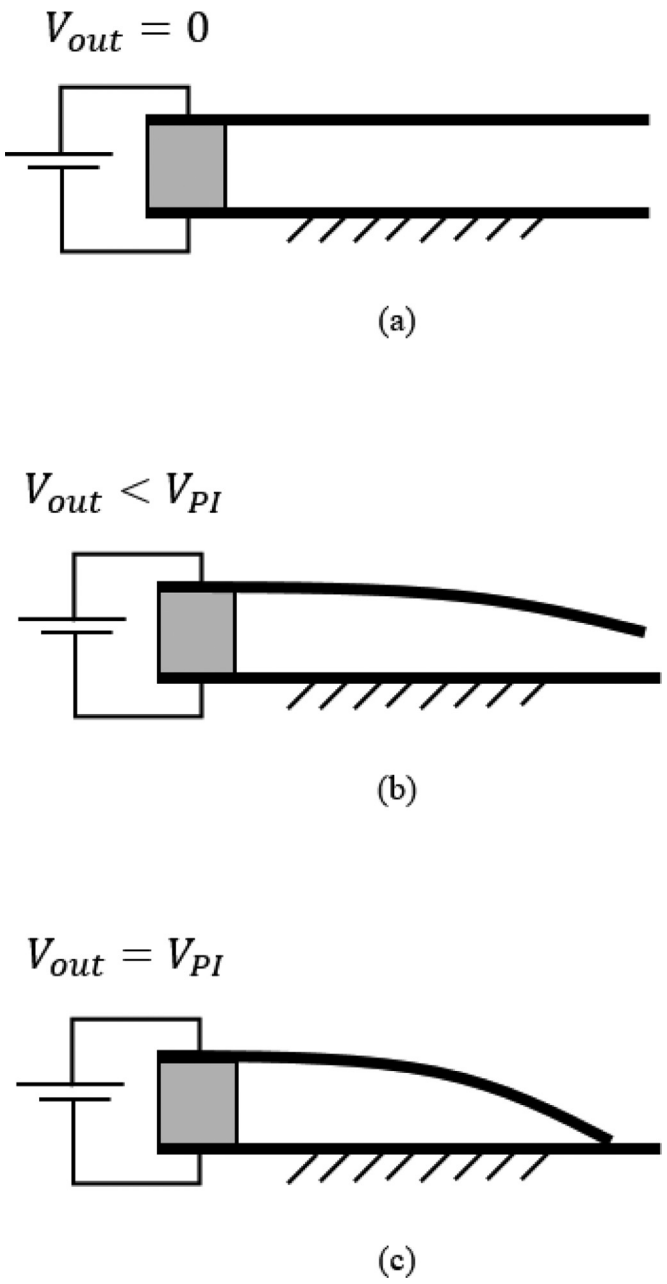

Fig. 1. The MEMS cantilever beam under different electrostatic voltage: no applied voltage (a), applied voltage lower than the critical pull-in limit (b), applied voltage at the pull-in (c).

take into account the dispersion forces of van deer Waals (vdW) and Casimir (Ramezani et al., 2006; Soroush et al., 2010). Both the intermolecular forces and the electrostatic actuation, influence the critical pull-in effects in MEMS-NEMS devices. Several numerical procedures and analytical methods can be traced in literature in order to estimate the pull-in parameters. The first approximated analytical approaches are the 1D based lumped model (Chowdhury et al., 2005), linearization methods (Noghrehabadi et al., 2012; Duan et al., 2013) or on Taylor series expansion of the loading term (Ghalambaz et al., 2011). In addition, numerical or approximate techniques to generate reduced-order models are used; the most popular methods are the differential quadrature method, Adomian decomposition method, Galerkin method and finite element method (Di Maida and Bianchi, 2016). On the other side, these approximated methods may provide large errors as the cantilever tip deflection increase closer to the pull-in stable position. Furthermore, these approaches give non-specified estimates of the pull-in stability parameters. By contrast, more accurate methods may provide the lower and upper bounds of the pull-in parameter, in order to ensure safely operating condition in the device. In particular, Radi et al. (2017), propose an accurate analytical approach for estimating the lower and upper bounds to the critical pull-in characteristics for microcantilever actuators. The proposed model aims to predict the critical factors, geometrical and electromechanical, of electrostatically microcantilever actuators that lead the transition between two stable positions. In a second work, Radi et al. (2018) consider the effect of the compressive axial load on the pull-in voltage, to obtain an accurate estimate of the stable actuating range. A variety of recent works on the pull-in analysis and modeling are reported in literature (Fakhrabadi et al., 2013; Krylov, 2007; De and Aluru, 2004; Nayfeh et al., 2005; Chaterjee and Pohit, 2009; Zhao et al., 2004; Bochobza-Degani and Nemirovsky, 2004; Luo and Wang, 2002). In summary, a review describing the pull-in instability phenomenon, modeling and analysis for MEMS-NEMS devices is represented by the review report of Zhang et al. (2014). Generally, every electromechanical device can be affected by pull-in instability (Somà, 2007): some devices rely on the pull-in instability for the switching operation such as sensor and actuators, while in other devices such as micro-mirrors and radio frequency oscillators the pull-in instability is an undesired effect (Van Beek and Puers, 2012; Juillard, 2015). This supports the need for a simple and accurate model to predict the critical pull-in voltage. One of the main practical limitation comes from the pull-in voltage value: on the one hand, low pull-in voltage reduces the power consumption but increases the uncontrolled switching deflection thus causing failure. On the other hand, high pull-in voltage allows to avoid undesired failure but increase the power consumption, thus enhancing the device performance. The pull-in instability effects and the mechanical response of these actuators are defined by three main issues. First, the choice of the material of the MEMS-NEMS devices and the modeling of the boundary support for the elastic structures (Noghrehabadi et al., 2013; Rinaldi et al., 2005), both for the static and dynamic/vibrational electrostatic simulation of the deflected beam. Second, the presence of dispersion of the intermolecular surface forces. The interaction forces of van deer Waals and Casimir depending on the gap separation between the two electrodes. As the gap decrease, namely below 20 nm for metals, the intermolecular forces becomes dominant, affecting the deflection and the stress-strain behavior of the nano-cantilever (Soroush et al., 2010; Ghalambaz et al., 2011). Third, the size dependency, also called size effect, that influences the mechanical properties of thecantilever when the size scale decrease rapidly (Stölken and Evans, 1998; Nix and Gao, 1998). With regard to the experimental characterization of the pull-in instability in MEMS devices, a number of proposal can be found in literature in order to evaluate the nonlinear static behavior of micro-electrostatic actuators (Somà et al., 2019; Ballestra et al., 2008). First experimental validation and analysis on the pull-in instability have been performed by Taylor (1968), Wickstrom and Davis (1967) and Siddique et al. (2011). Poelma et al. (2011) evaluates the pull-in phenomenon for electrostatically paddle cantilever from 3D imaging reconstruction. Alternatively, Somà focused on detecting the mechanical fatigue limits in response to the pull-in voltage actuation in gold micro-beams specimens (Somà and De Pasquale, 2009; Soma et al., 2017), and experimentally validated the residual stress in electrostatically actuated radio frequency micromechanical systems (RF-MEMS), (De Pasquale and Soma, 2007; Somà and Saleem, 2015). The understanding and control of the pull-in instability represents, even now, a great technological challenge (Zhang et al., 2014). As a consequence of the high cost in the implementation of miniaturized specimens, combined with the need of specific instrumentation, is not simple to examine the robustness of the theoretical predictions for different type of actuator configurations. However, analytical approaches consider negligible Casemir and vdW surface forces, when the dimension of the cantilever beams shift to the micro scale, and consequently, in the millimeter scale. This work focuses on the experimental characterization of the critical pull-in voltage and the tip deflection of a

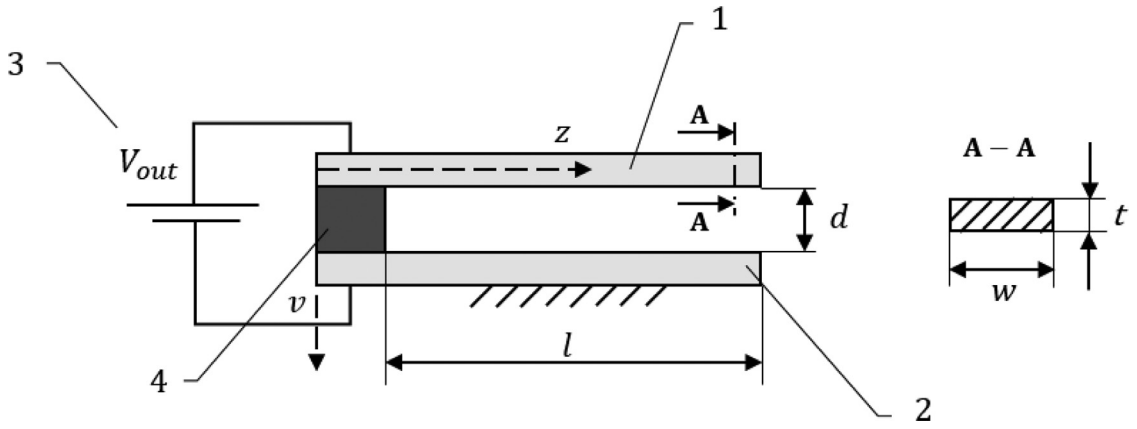

Fig. 2. The elastic micro-nano cantilever scheme subject to electrostatic actuation.

macro-scale size cantilever beam, with the aim to validate a theoretical micro-mechanical model proposed by Radi et al. (2017, 2018). Specifically, we designed and built a simple millimeter-scale cantilever, which was actuated through an ad-hoc electric circuit able to reproduce the same pull-in phenomenon observed in the micrometric scale. The tests investigated different cantilever configurations to examine the effect of the free length of the suspended electrode and the gap from the ground on the pull-in response. The proposed device is simply adaptable, low cost, and simple to manufacture. The experimental results exhibit a very good agreement with the analytical predictions (Radi et al., 2017, 2018). In particular, we obtained a relative difference between the experimental and analytical values of the pull-in voltage in the range between from 0.7% up to 10%, whereas the relative difference of the pull-in deflection falls in the range from 1.1% up to 18%.

2. Material and methods

Fig. 2 shows the configuration of the system examined in this work, which corresponds to the cantilever geometry and actuation scheme described in the works of Radi et al. (2017, 2018). Two plates compose the system: the flexible electrode (1), on top, and the ground (2), subject to an electrostatic actuation (3), and separated by a dielectric layer (4). In order to evaluate the variation of the pull-in factor voltage with respect to the geometrical dimensions of the device, we examined different cantilever configurations. In particular, we tested different lengths of the beam in combination with different gaps of the dielectric layer.

2.1. The macro-scale model

Fig. 2 shows the generic elastic micro/nano cantilever of length, l, width, w and thickness, t, clamped at one end, with $z = [0, l]$, and subject to electrostatic actuation and intermolecular surface forces (Radi et al., 2017, 2018). In particular, we considered the non-dimensional deflection, $u = v/d$, and the axial coordinate, $x = z/l$, where v is the deflection, and d is the initial gap between the two electrodes, respectively. The system can be described mathematically by the following fourth-order nonlinear ordinary differential equation (ODE):

$$u^{IV}(x) = \frac{\gamma\beta}{1-u(x)} + \frac{\beta}{[1-u(x)]^2} + \frac{\alpha_W}{[1-u(x)]^3} + \frac{\alpha_C}{[1-u(x)]^4} \tag{1}$$

$$u(0) = u'(0) = 0,\ u''(1) = u'''(1) = 0 \tag{2}$$

Where $\gamma = 0.65\ d/w$ is the fringing coefficient. Moreover, the non-dimensional positive parameters β, α_W and α_C are proportional to the electrostatic, van der Waals and Casimir forces, respectively, namely:

$$\beta = \frac{\varepsilon_0 w V^2 l^4}{2d^3 EI}$$

$$\alpha_W = \frac{Awl^4}{6\pi d^4 EI}$$

$$\alpha_C = \frac{\pi^2 hcwl^4}{240 d^5 EI} \tag{3}$$

Where $\varepsilon_0 = 8.854{*}10^{-12}\ C^2N^{-1}m^{-2}$ is the permittivity of vacuum, $h = 1.055{*}10^{-34}\ Js$ is the Plank's constant divided by 2π, $c = 2.998{*}10^8\ m/s$ is the speed of light, A is the Hamaker constant, V is the electric voltage applied to the electrodes, E is the Young's modulus of the beam material and I is the moment of inertia of the beam cross-section. As show in Eq. (3), the parameters β, α_W and α_C affected considerably the values of the pull-in instability factors and then the operation point of the device. In particular, when the dimensions of the cantilever beams increase, the values of the intermolecular force parameters α_W and α_C decrease, consequently, if the dimensions of the actuator shift to the millimeter-scale the effect of the van der Waals and Casimir forces becomes negligible (α_W and α_C values fall in the range of $10^{-25} \div 10^{-28}$). In this operating condition, named the "macro-scale condition", only the electrostatic force determines the pull-in instability threshold of the beam. In addition, for an elastic material with a specific Young's modulus, E, the value of the parameter β allows to predict the value of the pull-in voltage with fixed geometrical parameters, w, t and l. By changing the geometric ratio, γ, the value of β changes and consequently the pull-in actuation voltage, see Eq. (1). In particular, the pull-in voltage for the macro-scale actuated cantilever beam, which depend on β, can be expressed by the following formula:

$$V_{PI} = \sqrt{\beta \frac{2d^3 EI}{\varepsilon_0 wl^4}} \tag{4}$$

Where, $I = \frac{wt^3}{12}$, is the moment of inertia for a rectangular cross-section area.

The macro-scale cantilever beam is able to reproduce the same electro-mechanical behavior observed in the micrometric scale (Radi et al., 2017, 2018). In the present investigation, we focused on the macro-scale model, where the intermolecular forces are negligible. While keeping constant the ratio between the geometrical dimensions of the system, it is possible to obtain a macro-scale model of the cantilever by increasing the dimensions of the micro-system (Rollier et al., 2006). The corresponding critical pull-in deflection for the macro-scale model (Radi et al., 2017, 2018), named v_{PI}, fall in the range $44\% \div 55\%$ for a high fringing coefficient, specifically for $\gamma = 0 \div 3.25$, which corresponds to an air gap, d, five times greater than the width of the flexible beam, w (Soroush et al., 2010; Cheng et al., 2004; Ramezani et al., 2008). To simplify the experimental approach, the authors suggest these following approximated equations to compute the pull-in parameter considering the fringing field effect, β_{PI} for the pull-in voltage, and u_{PI} for the nor-

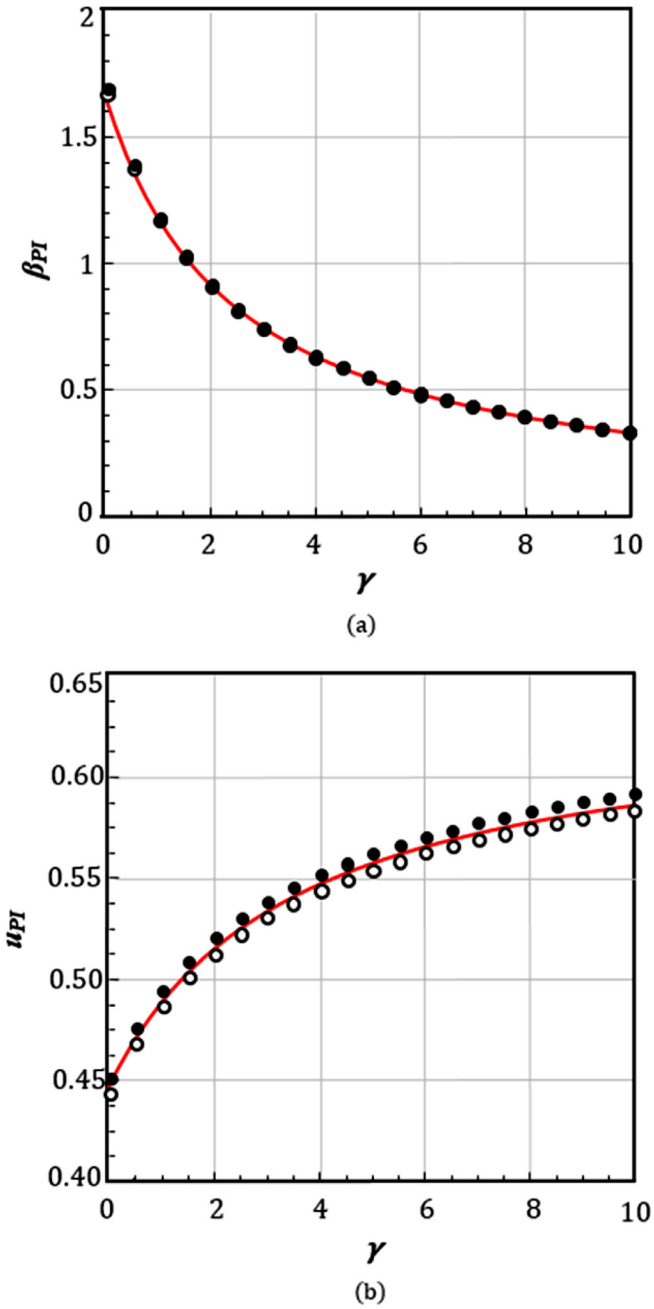

Fig. 3. The normalized pull-in voltage, β_{PI}, with respect to the variation of the fringing coefficient, γ (a), the normalized deflection u_{PI} with respect to γ (b). The continues curves represents the approximated solution, and the black dot and the empty circle the analytic estimate for the upper and lower bounds, respectively.

malized pull-in deflection:

$$\beta_{PI} = \frac{1.67}{1+0.41\gamma}$$
$$u_{PI} = 0.6395 - \frac{2084}{10862+3069\gamma} \tag{5}$$

Using the analytical procedure described in Radi et al. (2017, 2018), lower and upper bounds are obtained for the pull-in parameters. Then, these estimates are used to fit the coefficients of the approximated relations (Eq. (5)) using the interpolation method available in Mathematica (Wolfram Research Inc 2020). The approximated curves fit very well with the lower and upper estimates of the pull-in voltage (Fig. 3a) and deflection (Fig. 3b) respectively, thus ensuring the accuracy of the approximated Eq. (5). Moreover, the approximated Eq. (5) for the voltage β_{PI} perfectly agrees with the approximated model introduced by Osterberg and Senturia (1997) and Ballestra et al. (2008).

2.2. Prototype development

First, the work focused on the design and prototype development of an adaptable millimeter-scale model of the MEMS device. The system is composed by two different parts: the mechanical one, formed by the switching system, the actuated cantilever, and the electrical part consisting of an electric circuit that regulates the input actuation on the device. In particular, the implemented device includes different pins output for the connection to the signal acquisition and monitoring system that registers the electrostatically response of the system.

2.3. Actuated cantilever

The dimensions of the macro-scale model, and the related pull-in factors of the system, are affected by the geometric aspect ratios of the electrodes and by the value of the gap. From the work of Rollier et al. (2006), it is possible determine the cantilever's parameters relating to a system described by the Euler's theory, where, the geometric aspect ratios of the plates are represented by:

$$R_1 = \frac{w}{l}$$
$$R_2 = \frac{d}{l}$$
$$R_3 = \frac{t}{l}$$
$$R_4 = \frac{t}{w} \tag{6}$$

As show in the work of Ballestra (Ballestra et al., 2008), by keeping constant the ratio R_4, the value of the pull-in voltage and deflection is affected by the values of the total free length of the flexible electrode, l, and from the gap, d. The increase in the scale, corresponds an increase of the voltage actuation for the cantilever beam. For this reason, a preliminary analysis of pull-in voltage and deflection was conducted with the aim to identify possible cantilever lengths, l, and predict the maximum pull-in voltage for different beam configurations (see Section 2.6 "Test plan"). Hence, the maximum admissible pull-in voltage was set, for the macro-scale model, at 3000 V, for a gap, d, in the range between 0.5 and 1 mm. Fig. 4 shows the case of planar plates with constant R_4. The switching system is composed of two plates with a rectangular cross-sectional area, the suspended and flexible electrode, and the fixed ground, both made of steel C100S with nominal Young's modulus, $E = 210,000\ MPa$, and a Poisson's ratio, ν, equal to 0.3. The electrodes of the system are simply obtained from a commercial steel tape, with the aim to have planar and lightweight beams. The plates of the system have a thickness, $t = 0.2\ mm$, and a width, $w = 12.7\ mm$, which correspond to an $R_4 = 0.0157$. The free length, l, of the suspended electrode was set initially equal to 50 mm, while the gap between the two electrodes was set equal to 0.6 mm and obtained through a simple bi-adhesive tape (Fig. 4), which makes easier the assembly of the flexible electrode on the dielectric support. The flexible electrode was placed on the bi-adhesive tape by pliers and then, the gap height d, was measured by an altimeter. From the analytical model of Radi et al. (2017, 2018), it is possible to calculate the pull-in parameter β of the system (see Eqs. (1) and (5)) for fixed w, t, l and d and the corresponding analytical pull-in voltage, V_{PI} (see Eq. (4)).

2.4. Power circuit

Due to the macro scale, the device requires a high actuation voltage to reach the pull-in. For this reason, we used a high voltage DC-DC converter (*EMCO CB101*) powered at 12 V through a power supply and

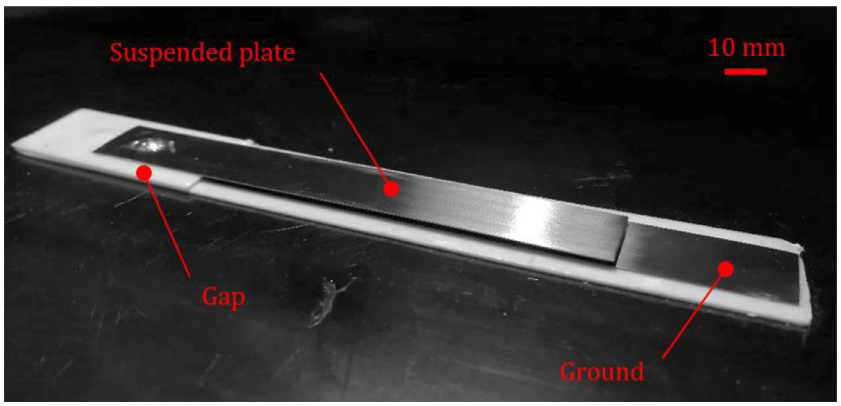

Fig. 4. Millimeter scale device implemented.

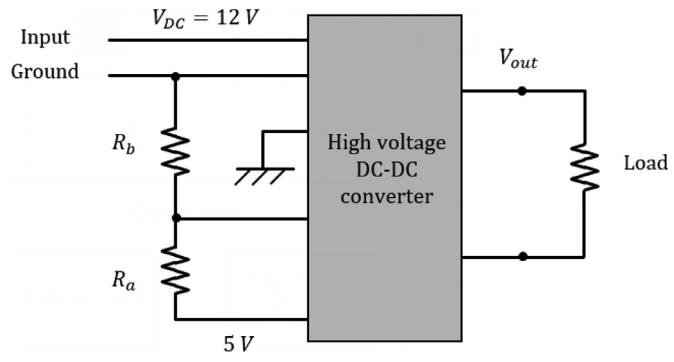

Fig. 5. The operating circuit of the converter.

giving an output voltage, V_{out}, in a range between 0 and $\pm 10\ kV$. Fig. 5 shows the operating circuit of the device.

Specifically, we have the high voltage DC-DC converter, and a simple circuit that allows to regulate the output voltage, V_{out}, which is the actuation voltage for the flexible cantilever. The regulation circuit consists of a voltage divider with electric resistances, R_a and R_b. Based on the schematic in Fig. 5, the output voltage of the device, V_{out}, is related to the value of the resistances R_a and R_b (Fig. 5) through the following equation:

$$V_{out} = \frac{R_a}{R_a + R_b} * (10,000) \tag{7}$$

By keeping a high value for R_b, about 10 $k\Omega$, the corresponding V_{out} of the converter is provided by the value of R_a. By replacing the two resistors R_a and R_b with a manual multi-turn potentiometer, we can regulate the output voltage from the DC-DC converter, from 0 up to the pull-in threshold, V_{PI}, thus, the corresponding output voltage, V_{out}, can be computed by Eq. (7). The critical value of the output voltage corresponds to the pull-in voltage, V_{PI}, as mentioned in Section 1. The high voltage output pin of the converter is finally connected on the top surface of the suspended electrode where the macro-beam is bonded. Fig. 6 shows the implemented electric circuit solution that includes all the electrical components of the power circuit, that are the DC-DC converter and the potentiometer. It is remarkable that the value of the current trough the circuit is maintained very low, about 200 mA, far below the possible critical value for failure. When pull-in occurs, the high voltage converter turns off, avoiding high electric charge on the circuit.

2.5. Experimental set-up

The experimental validation aims to measure the critical pull-in voltage and deflection of the cantilever beam. Fig. 7 shows the schematic of the test bench for the experimental validation.

In order to measure the tip deflection of the suspended electrode, we used a single point laser-doppler vibrometer (Polytec OFV-505 sensor head) with a tolerance on the position of 0.002 mm. The vibrometer points to the tip of the flexible electrode, in the vertical direction with respect to the initial top surface of the flexible electrode (Immovilli et al., 2013, 2011), Fig. 7. The vibrometer is managed by a National Instrument data acquisition board (NI 9211). The acquisition board also measure the pull-in voltage connected to the device. Before applying the actuation voltage to the device, we ensured that the beams were discharged, in order to avoid early pull-in phenomenon due to residual electrical charge in the electrodes. When the power circuit is on, the flexible micro-cantilever beam deflects towards to the substrate under the action of the electrostatic forces provided by the high voltage converter, and the vibrometer simultaneously and continuously recorded the corresponding tip deflection, until the system reached the pull-in. The slow regulation of the input voltage thanks to the potentiometer, prevented voltage fluctuation during the actuation of the system and thus made possible to acquire the effective pull-in voltage of the beam. The acquisition board was connected to a PC that registered and processed the data using an algorithm implemented in the LabVIEW environment (Bitter et al., 2020).

2.6. Test plan

In order to assess the accuracy of the prototype, we tested some different configurations of the cantilever to examine the influence of some parameters on the pull-in. For this investigations we considered constant nominal width, $w = 12.7\ mm$, as reported in the work of Ballestra et al. (2008), and nominal thickness, $t = 0.2\ mm$, for all the specimens tested (see Section 2.3 "Actuated cantilever"). Specifically, we investigated three levels of free length, l, in combination with two different gaps from the ground, d. Table 1 reports the six cantilever configurations investigated experimentally. For all the six configurations in Table 1, we performed ten replications of the pull-in tests, for a total of 60 tests. Each of the six configurations tested was manufactured as a completely new specimen.

3. Results

Table 2 compares the critical pull-in parameters for the six configurations investigated (see Table 1) where, V_{PI}^{E} and V_{PI}^{A}, represent the experimental and the analytical pull-in voltages, respectively, and $v_{\mathrm{PI}}^{\mathrm{E}}$ and $v_{\mathrm{PI}}^{\mathrm{A}}$ the corresponding pull-in deflections, using the analytical model provided by Radi et al. (2017, 2018).

In particular, for the experimental pull-in voltage and deflection, we reported the mean value and the corresponding standard deviation for the 10 replications performed. Figs. 8 and 9 show, respectively, the relation between the experimental pull-in voltage, V_{PI}^{E}, and the deflection, $v_{\mathrm{PI}}^{\mathrm{E}}$, with respect to the variation of the gap, d, and of the total free length, l.

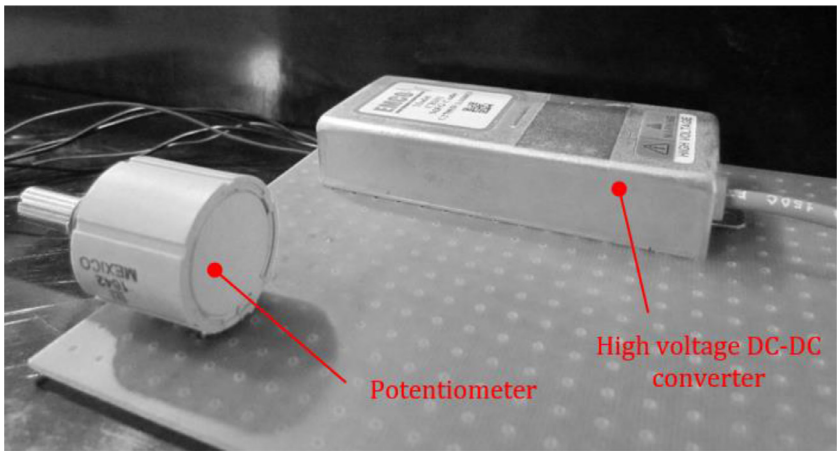

Fig. 6. The electric board and the converter circuit implemented.

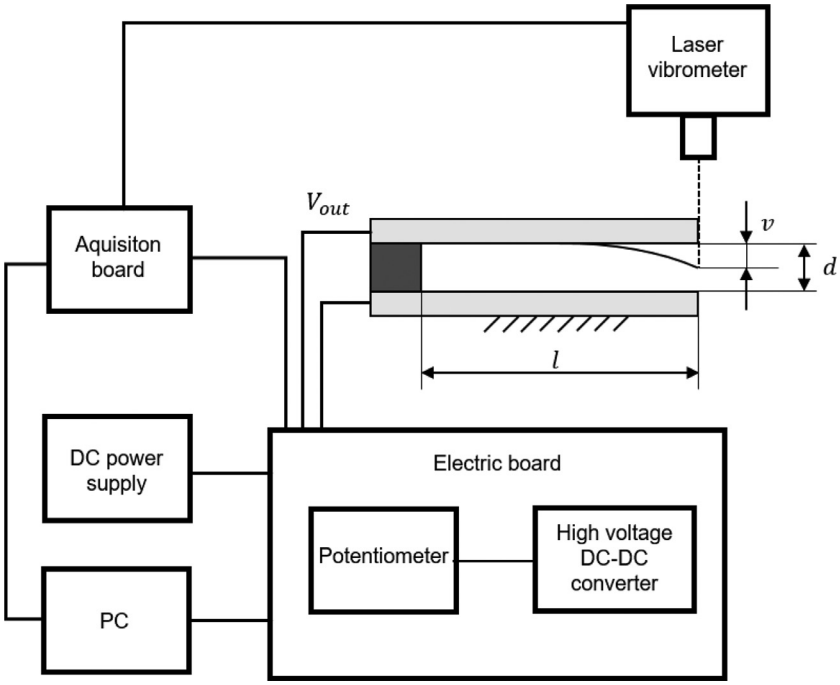

Fig. 7. Schematic of the testing benchmark.

Table 1
Nominal dimensions and related aspect ratios for the different specimens tested.

Specimen	l [mm]	w [mm]	t [mm]	d [mm]	R_1	R_2	R_3	R_4
1	50.00±0.02	12.7	0.2	0.60±0.02	0.254	0.012	0.004	0.016
2	60.00±0.02	12.7	0.2	0.60±0.02	0.212	0.01	0.003	0.016
3	70.00±0.02	12.7	0.2	0.60±0.02	0.181	0.009	0.003	0.016
4	50.00±0.02	12.7	0.2	0.80±0.02	0.254	0.016	0.004	0.016
5	60.00±0.02	12.7	0.2	0.80±0.02	0.212	0.013	0.003	0.016
6	70.00±0.02	12.7	0.2	0.80±0.02	0.181	0.011	0.003	0.016

The critical pull-in values obtained experimentally and analytically are compared to the value of the critical pull-in factors obtained numerically by the shooting method (Osborne, 1969) implemented in the Mathematica software Mathematica (Wolfram Research Inc 2020). The diagrams in Figs. 10 and 11 relate the pull-in voltage, y axis of the graph, and the pull-in deflection, x axis of the graph, for the two different gaps considered.

4. Discussion

As shown in Figs. 8 and 9 it appears that both the variable free length, l, and the value of the gap, d, of the device affected the amount of the pull-in voltage significantly: on the one hand, the higher the length of the flexible electrode, l, the higher the value of the pull-in voltage. On the other hand, by decreasing the value of the gap, d, the pull-in voltage decreases according to the analytical prediction model (Radi et al., 2017, 2018). The experimental results in Table 2 exhibit a very good agreement with the analytical predictions from the model proposed by Radi et al. (2017, 2018). In particular, the relative difference between the experimental measurements and analytical values of the pull-in voltage falls in the range between 0.7% and 10%, whereas the relative difference for the pull-in deflection falls in the range from 1.1% up to 18% (Table 2). In addition, Figs. 10 and 11 highlight that the pull-in critical values provided by the shooting method (Osborne, 1969) closely match

Table 2
Comparison between the experimental and analytical pull-in voltage and tip deflection.

Specimen	V_{PI}^{E} [V]	V_{PI}^{A} [V]	v_{PI}^{E} [mm]	v_{PI}^{A} [mm]
1	1261 ± 19	1337	0.262 ± 0.024	0.268
2	891 ± 42	929	0.263 ± 0.018	0.268
3	682 ± 25	682	0.273 ± 0.018	0.268
4	2047 ± 28	2052	0.298 ± 0.050	0.357
5	1423 ± 16	1425	0.359 ± 0.028	0.357
6	942 ± 93	1047	0.391 ± 0.016	0.357

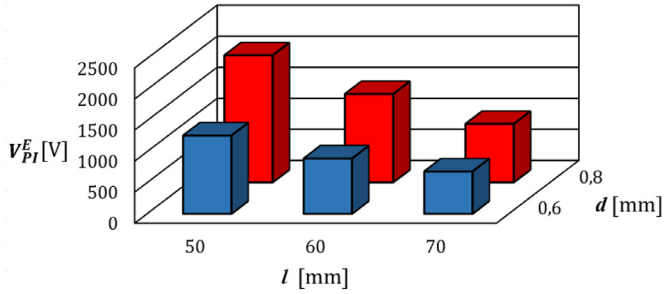

Fig. 8. The experimental pull-in voltage variation for the different cases evaluated.

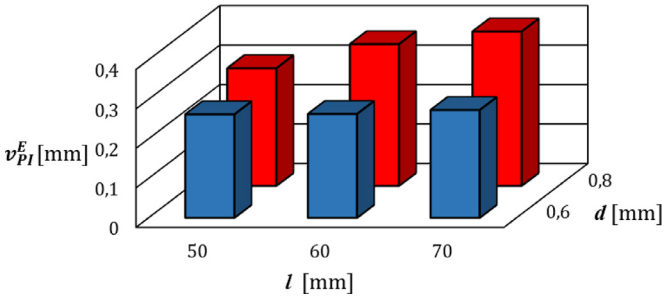

Fig. 9. The experimental pull-in deflections measured.

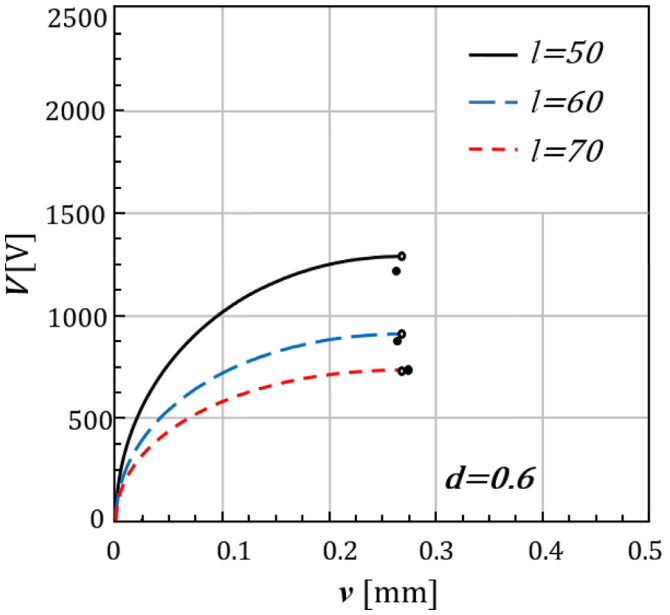

Fig. 10. The pull-in voltage, V_{PI}, with respect to the deflection,v, for different free lengths, l, and for a fixed gap, d, equal to 0.6 *mm*. The solid lines represent the numerical solution, the black dots the experimental estimates, and the white circles the analytical estimates, respectively.

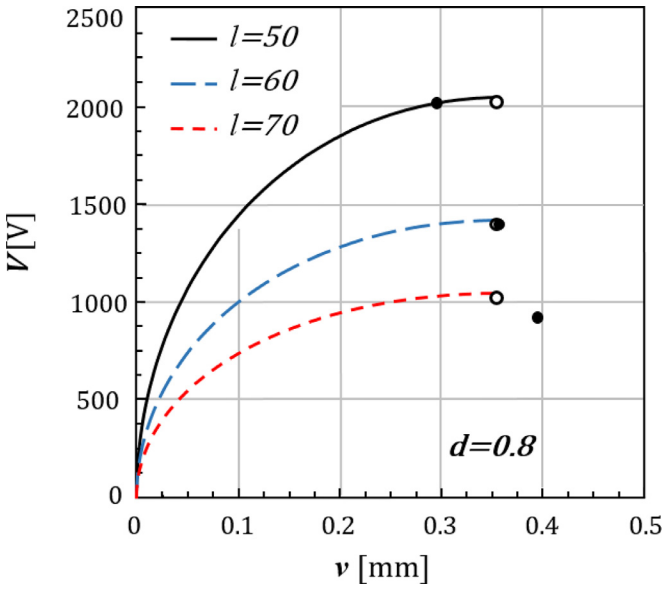

Fig. 11. The pull-in voltage, V_{PI}, with respect to the variation of the deflection,v, for different free length, l, and for fixed gap, d, equal to 0.8 *mm*. The solid lines represent the numerical solution, the black dots the experimental estimates, and the white circles the analytical estimates, respectively.

the experimental measurements. From Table 2, we can observe a significant scatter in the values of the pull-in voltage and deflection, that can be imputed to the following geometrical issues. First, the combined effect of the inaccuracies in the air gap, d, and in the free length, l, of the experimental device: for instance, according to the analytical model (Eqs. (4) and (5)), a 0.01 *mm* variation in the gap, d, combined with a 0.1 *mm* variation of the free length, l, give a scatter of the pull-in voltage from about 20 up to 47 V. Second, small inaccuracies in the positioning of the mobile plate on the bi-adhesive gap gives not perfect alignment on the clamped cantilever thus affecting the planarity between the two electrodes. Third, the higher the free length, l, the higher the effect of the weight of the flexible plate, see Table 2. Nevertheless, the proposed analytical model by Radi et al. (2017, 2018), gives an accurate prediction of the experimental behavior of the system, also compared to previous works in the literature (Ballestra et al., 2008) and Rollier et al., 2006). The proposed macro-scale model is a low-cost solution with the only limitation of a high actuation voltage to reach the pull-in threshold (Table 2). With regard to prototype manufacturing, the proposed solution has the following advantages. First, the macro scale prototype is more simple and quick to set-up, compared to a micro-nano scale solution. Second, by changing the cantilever configuration, it is possible to test different macro-scale models, thanks to the fact that the electric board of the prototype is external and isolated form the switching part. Third, the macro-scale prototype implemented allows to recreate the same switching phenomenon observed in the nano scale, with exception of the Casimir and vdW surface forces. In addition, considering the fringing effect in the analytical model also for the macro-scale solution (Eqs. (4) and (5)), the experimental results show a remarkable improvement compared to the models in the literature, see Figs. 10 and 11.

5. Conclusions

The present work assesses a previous analytical model from the literature via experimental tests with the use of a simple millimeter-scale device, which was actuated through an ad-hoc electric circuit. The work aimed to measure the critical pull-in voltage and the deflection of an actuated cantilever beam for different configurations in order to validate the variation of the pull-in voltage with the geometrical parameters

of the device provided by theoretical investigations. Analytical predictions closely match the experimental estimates, where the maximum relative difference between experimental and analytical values of the pull-in voltage is in the order of 10%, whereas the relative difference of the pull-in deflection falls below 18%. The adaptable prototype developed allowed to evaluate different cantilever configurations, then, the influence of the geometrical and electromechanical parameters for the system on the pull-in instability. The proposed macro-scale prototype is a very quick and smart solution from a manufacturing standpoint.

Funding

This research did not receive any specific grant from funding agencies in the public, commercial, or not-for-profit sectors.

Declaration of Competing Interest

All authors agree on the submission of the paper in the present form.

References

Ballestra, A., Brusa, E., Munteanu, M.G., et al., 2008. Experimental characterization of electrostatically actuated in-plane bending of microcantilevers. Microsyst. Technol. 14, 909–918.

Bitter R., Mohiuddin T., Nawrocki M. 2020 Labview: Advanced Programming Techniques.

Bochobza-Degani, O., Nemirovsky, Y., 2004. Experimental verification of a design methodology for torsion actuators based on a rapid pull-in solver. J. Microelectromech. Syst. 13, 121–130.

Chaterjee, S., Pohit, G., 2009. A large deflection model for the pull-in analysis of electrostatically actuated microcantilever beams. J. Sound Vib. 322, 969–986.

Cheng, J., Zhe, J., Wu, X., 2004. Analytical and finite element model pull-in study of rigid and deformable electrostatic microactuators. J. Micromech. Microeng. 14, 57–68.

Chowdhury, S., Ahmadi, M., Miller, W.C., 2005. A closed-form model for the pull-in voltage of electrostatically actuated cantilever beams. J. Micromech. Microeng. 15, 756–763.

Chuang, W.C., Lee, H.L., Chang, P.Z., et al., 2010. Review on the modeling of electrostatic MEMS. Sensors 10, 6149–6171.

De, S.K., Aluru, N.R., 2004. Full-Lagrangian schemes for dynamic analysis of electrostatic MEMS. J. Microelectromech. Syst. 13, 737–758.

De Pasquale, G., Soma, A., 2007. Design and finite element simulation of MEMS for fatigue test. In: Proceedings of the International Semiconductor Conference, 1. CAS, pp. 159–162.

Dequesnes, M., Rotkin, S.V., Aluru, N.R., 2002. Calculation of pull-in voltages for carbon–nanotube-based nanoelectromechanical switches. Nanotechnology 13, 120–131.

Di Maida, P., Bianchi, G., 2016. Numerical investigation of pull-in instability in a micro-switch MEMS device through the pseudo-spectral method. Model. Simul. Eng. doi:10.1155/2016/8543616, Epub ahead of print 2016.

Duan, J.S., Rach, R., Wazwaz, A.M., 2013. Solution of the model of beam-type micro- and nano-scale electrostatic actuators by a new modified Adomian decomposition method for nonlinear boundary value problems. Int. J. Non Linear Mech. 49, 159–169.

Eric Garfunkel A.D.*Advanced Materials and Technologies for Micro / Nano-Devices, Sensors and Actuators NATO Science for Peace and Security Series*. 2009.

Espinosa H.D., Ke C., Pugno N.*Nanoelectromechanical Systems: Experiments and Modeling*. 2006. Epub ahead of print 2006. doi:10.1016/b0-08-043152-6/02134-3.

Fakhrabadi, M.M.S., Khorasani, P.K., Rastgoo, A., et al., 2013. Molecular dynamics simulation of pull-in phenomena in carbon nanotubes with Stone-Wales defects. Solid State Commun. 157, 38–44.

Ghalambaz, M., Noghrehabadi, A., Abadyan, M., et al., 2011. A new power series solution on the electrostatic pull-in instability of nano cantilever actuators. Proc. Eng. 10, 3708–3716.

Gorthi, S., Mohanty, A., Chatterjee, A., 2006. Cantilever beam electrostatic MEMS actuators beyond pull-in. J. Micromech. Microeng. 16, 1800–1810.

Immovilli, F., Bianchini, C., Cocconcelli, M., et al., 2011. Currents and vibrations in asynchronous motor with externally induced vibration. In: Proceedings of the SDEMPED 2011 - 8th IEEE Symposium on Diagnostics for Electrical Machines, Power Electronics and Drives, pp. 580–584.

Immovilli, F., Bianchini, C., Cocconcelli, M., et al., 2013. Bearing fault model for induction motor with externally induced vibration. IEEE Trans. Ind. Electron. 60, 3408–3418.

Ionescu, A.M., 2015. Nano-Electro-Mechanical (NEM) memory devices. Emerg. Nanoelectron. Devices 9781118447, 123–136.

Juillard, J., 2015. Analysis of resonant pull-in of micro-electromechanical oscillators. J. Sound Vib. 350, 123–139.

Ke, C.H., Pugno, N., Peng, B., et al., 2005. Experiments and modeling of carbon nanotube-based NEMS devices. J. Mech. Phys. Solids 53, 1314–1333.

Knapp, J.A., De Boer, M.P., 2002. Mechanics of microcantilever beams subject to combined electrostatic and adhesive forces. J. Microelectromech. Syst. 11, 754–764.

Krylov, S., 2007. Lyapunov exponents as a criterion for the dynamic pull-in instability of electrostatically actuated microstructures. Int. J. Non Linear Mech. 42, 626–642.

Loh, O.Y., Espinosa, H.D., 2012. Nanoelectromechanical contact switches. Nat. Nanotechnol. 7, 283–295.

Luo, A.C.J., Wang, F.Y., 2002. Chaotic motion in a micro-electro-mechanical system with non-linearity from capacitors. Commun. Nonlinear Sci. Numer. Simul. 7, 31–49.

Nayfeh, A.H., Younis, M.I., Abdel-Rahman, E.M., 2005. Reduced-order models for MEMS applications. Nonlinear Dyn. 41, 211–236.

Nix, W.D., Gao, H., 1998. Indentation size effects in crystalline materials: a law for strain gradient plasticity. J. Mech. Phys. Solids 46, 411–425.

Noghrehabadi, A., Ghalambaz, M., Ghanbarzadeh, A., 2012. A new approach to the electrostatic pull-in instability of nanocantilever actuators using the ADM-Padé technique. Comput. Math. Appl. 64, 2806–2815.

Noghrehabadi, A., Eslami, M., Ghalambaz, M., 2013. Influence of size effect and elastic boundary condition on the pull-in instability of nano-scale cantilever beams immersed in liquid electrolytes. Int. J. Non Linear Mech. 52, 73–84.

Osborne, M.R., 1969. On shooting methods for boundary value problems. J. Math. Anal. Appl. 27, 417–433.

Osterberg, P.M., Senturia, S.D., 1997. M-test: a test chip for MEMS material property measurement using electrostatically actuated test structures. J. Microelectromech. Syst. 6, 107–118.

Passian, A., Thundat, T., 2011. Chapter 2262 - Microcantilever Sensors. Encycl. Mater. Sci. Technol. (Second Edition), 1–6. doi:10.1016/B978-0-08-043152-9.02262-4.

Poelma, R.H., Sadeghian, H., Noijen, S.P.M., et al., 2011. A numerical experimental approach for characterizing the elastic properties of thin films: application of nanocantilevers. J. Micromech. Microeng. 21. doi:10.1088/0960-1317/21/6/065003, Epub ahead of print.

Radi, E., Bianchi, G., di Ruvo, L., 2017. Upper and lower bounds for the pull-in parameters of a micro- or nanocantilever on a flexible support. Int. J. Non Linear Mech. 92, 176–186.

Radi, E., Bianchi, G., di Ruvo, L., 2018. Analytical bounds for the electromechanical buckling of a compressed nanocantilever. Appl. Math. Model. 59, 571–582.

Ramezani, A., Alasty, A., Akbari, J., 2006. Influence of van der Waals force on the pull-in parameters of cantilever type nanoscale electrostatic actuators. Microsyst. Technol. 12, 1153–1161.

Ramezani, A., Alasty, A., Akbari, J., 2008. Closed-form solutions of the pull-in instability in nano-cantilevers under electrostatic and intermolecular surface forces. Int. J. Solids Struct. 45, 2598–2612.

Rinaldi, G., Packirisamy, M., Stiharu, I., 2005. Multi-parameter synthesis of microsystems. Photonic Appl. Devices Commun. Syst. 5970, 597016.

Rollier, A.S., Legrand, B., Collard, D., et al., 2006. The stability and pull-in voltage of electrostatic parallel-plate actuators in liquid solutions. J. Micromech. Microeng. 16, 794–801.

Siddique, J.I., Deaton, R., Sabo, E., et al., 2011. An experimental investigation of the theory of electrostatic deflections. J. Electrostat. 69, 1–6.

Somà, A., De Pasquale, G., 2009. MEMS mechanical fatigue: experimental results on gold microbeams. J. Microelectromech. Syst. 18, 828–835.

Somà, A., Saleem, M.M., 2015. Modeling and experimental verification of thermally induced residual stress in RF-MEMS. J. Micromech. Microeng. 25, 55007.

Somà, A., Saleem, M.M., Margesin, B., et al., 2019. Pull-in tests of MEMS specimens for characterization of elastic–plastic behavior. Microsyst. Technol. 4396.

Somà, A., 2007. MEMS Design for reliability: mechanical failure modes and testing. Perspect. Technol. Methods MEMS Des. 0, 296.

Soma, A., Saleem, M.M., Margesin, B., 2017. Experimental characterization of elastic-plastic behavior of MEMS electroplated gold specimens. In: Proceedings of the Symposium on Design, Test, Integration and Packaging of MEMS/MOEMS, DTIP, 2017 doi:10.1109/DTIP.2017.7984501, Epub ahead of print.

Soroush, R., Koochi, A., Kazemi, A.S., et al., 2010. Investigating the effect of Casimir and van der Waals attractions on the electrostatic pull-in instability of nano-actuators. Phys. Scr. 82. doi:10.1088/0031-8949/82/04/045801, Epub ahead of print.

Spaggiari A., Castagnetti D., Golinelli N., et al. Smart Materials : Properties, Design and Mechatronic Applications. 2016; 0: 1–29.

Stölken, J.S., Evans, A.G., 1998. A microbend test method for measuring the plasticity length scale. Acta Mater. 46, 5109–5115.

Taylor, G., 1968. A PRSL. The coalescence of closely spaced drops when they are at different electric potentials. In: Proceedings of the Royal Society of London Series A Mathematical and Physical Sciences, 306, pp. 423–434.

Van Beek, J.T.M., Puers, R., 2012. A review of MEMS oscillators for frequency reference and timing applications. J. Micromech. Microeng. 22. doi:10.1088/0960-1317/22/1/013001, Epub ahead of print.

Wickstrom, R.a., Davis, J.R., 1967. Gate transistor. IEEE Trans. Electron Devices 14, 117–133.

Wolfram Research Inc. 2020 Mathematica 9.0.

Zhang, W.M., Yan, H., Peng, Z.K., et al., 2014. Electrostatic pull-in instability in MEMS/NEMS: a review. Sens. Actuators A 214, 187–218.

Zhao, X., Abdel-Rahman, E.M., Nayfeh, A.H., 2004. A reduced-order model for electrically actuated microplates. J. Micromech. Microeng. 14, 900–906.